

Fe₃O₄, FeCO₃ or FeS - Which Corrosion Product Will Prevail at High Temperature in CO₂/H₂S Environments?

Shujun Gao, Bruce Brown, David Young, Srdjan Nestic, Marc Singer
Institute for Corrosion and Multiphase Technology,
Department of Chemical & Biomolecular Engineering, Ohio University
342 West State Street
Athens, OH, 45701
USA

ABSTRACT

Sweet (CO₂) and sour (H₂S) corrosion have continuously been a challenge in oil and gas production and transportation. Yet, some key issues are still not well understood, especially at high temperature production conditions. A CO₂/H₂S ratio of 500, which has been used (often inaccurately) to determine which corrosion mechanism is dominant, is probably even less valid at high temperature. The nature of the corrosion products forming at high temperature in CO₂/H₂S environments and their effects on the corrosion rate are not known. Finally, the impact on pipeline integrity of environmental changes between sweet and sour production conditions (simulating reservoir souring) has not been well documented. CO₂, H₂S, and CO₂/H₂S corrosion experiments were conducted at 120°C to investigate corrosion mechanisms and corrosion product layer formation at high temperature. The results show that the corrosion products were still clearly dominated by H₂S under the pCO₂/pH₂S ratio of 550. Formation of Fe₃O₄, FeCO₃, and FeS corrosion product layers had a direct impact on the measured corrosion rates and was dependent on the gas composition and on the sequence of exposure (CO₂ then H₂S and *vice versa*). Compared with H₂S corrosion alone, the presence of CO₂ could retard Fe₃O₄ formation in CO₂/H₂S mixture environment. No obvious change in steady state corrosion rate was observed when the corrosion environment was switched from CO₂ to H₂S and *vice versa*.

Key words: high temperature corrosion, CO₂/H₂S, iron oxide, iron carbonate, iron sulfide

INTRODUCTION

Carbon dioxide (CO₂) and hydrogen sulfide (H₂S) are the two acid gases that are commonly associated with oil and gas industry. The presence of CO₂, H₂S, and free water can cause severe internal corrosion problems in wells and pipelines, which poses serious challenges to process safety, equipment integrity, eco-system and human health.¹⁻³ Moreover, corrosion environments become ever harsher as more and more wells are drilled to deeper depths that contain oil and gas at high temperature and high pressure (HTHP) conditions.⁴⁻⁶

CO₂ and H₂S corrosion have been widely studied and significant progress has been made in the past decades in determining the controlling mechanisms.⁷⁻¹⁰ However, there are still some key issues that are poorly understood, especially when it comes to high temperature, as described in the following text.

In 1983, Dunlop *et al.*,¹¹ proposed a CO₂/H₂S ratio of 500 to determine whether the corrosion would be dominated by CO₂ or H₂S at 25°C. This ratio has been widely quoted and applied in other industry documents.¹²⁻¹³ However, its validity has also been challenged if used under different conditions at 25°C.¹⁴ In addition, the terminology used to determine which gas will have a “dominant” effect on corrosion is very confusing. Whether it is based on the argument of “corrosion rate” or “corrosion product” is still unclear. Consequently, how this ratio can be applied in deciding which mitigation method, steel type or corrosion prediction tool to use still remains uncertain. A simple question to address here is whether or not the CO₂/H₂S ratio of 500 is valid at high temperature (research question #1). While the answer to this question is obviously “no”, a reflection on the validity of a simple critical CO₂/H₂S ratio is still useful.

Previous studies have shown that Fe₃O₄ can form in both CO₂ and H₂S environments at high temperatures.¹⁵⁻¹⁸ Generally, Fe₃O₄ formed at high temperature can be considered as a protective layer.¹⁹ However, in a recent experimental study performed at high temperatures using an autoclave, the uniform steady state corrosion rate in “CO₂-only” environment was around 0.1 mm/yr,¹⁵ while that in an “H₂S-only” environment was shown to be approximately 2 mm/yr¹⁶. Why was a much higher corrosion rate observed in an “H₂S-only” environment (research question #2)?

Most studies focus on CO₂ or H₂S corrosion alone,²⁰⁻²³ or mixed CO₂/H₂S corrosion.^{24,25} Little is known when the corrosion environment switches from sour (H₂S) to sweet (CO₂) or from sweet to sour. For example, CO₂ gas can be injected into a sour reservoir to reduce the oil viscosity and enhance the oil recovery.²⁶ Similarly, if H₂O is injected into a sweet well, some microorganisms such as sulfate reducing bacteria (SRB) can be developed and produce H₂S.²⁷ What is the impact of this environmental change on pipeline integrity? Can aged pipeline still be used or do they need to be replaced?²⁸ Therefore, it is necessary to investigate the corrosion behavior of mild steel with environmental change from sweet to sour and *vice versa* (research question #3).

In order to address the above stated three research questions, CO₂ and/or H₂S corrosion experiments were conducted at 120°C. Linear polarization resistance (LPR), X-ray diffraction (XRD), and scanning electron microscopy with energy dispersive X-ray spectroscopy microanalysis (SEM/EDS) methods were employed to investigate the validity of the CO₂/H₂S = 500 ratio, the role of the Fe₃O₄ layer in corrosion, and the effect of environmental transitions.

EXPERIMENTAL PROCEDURE

High temperature experiments were carried out in a 7 L Hastelloy[†] autoclave, as shown in **Error! Reference source not found.** Linear polarization resistance (LPR) measurements were conducted using a conventional three-electrode configuration. The working electrode was a cylindrical API 5L X65 mild steel, whose chemical composition is shown in Table 1. Due to the lack of a reliable reference electrode at high temperature in an H₂S environment, a commercial Zr/ZrO₂ high temperature, high pressure pH probe was used as a pseudo reference electrode. It could serve as a reference electrode as long as its potential was stable under the operating conditions, but the exact potential was still unknown.²⁹ The counter electrode was a Pt-coated Nb cylinder. LPR corrosion rate was measured about every two hours at a scan rate of 0.125 mV/s between ±5 mV vs. OCP. Some square X65 specimens were also hung on a stabilized shaft for additional analysis. A central impeller, with a 1000 rpm rotating speed, was used to well mix the solution during the experiment. The electrolyte was 1 wt.% NaCl aqueous solution.

[†] Trade Name

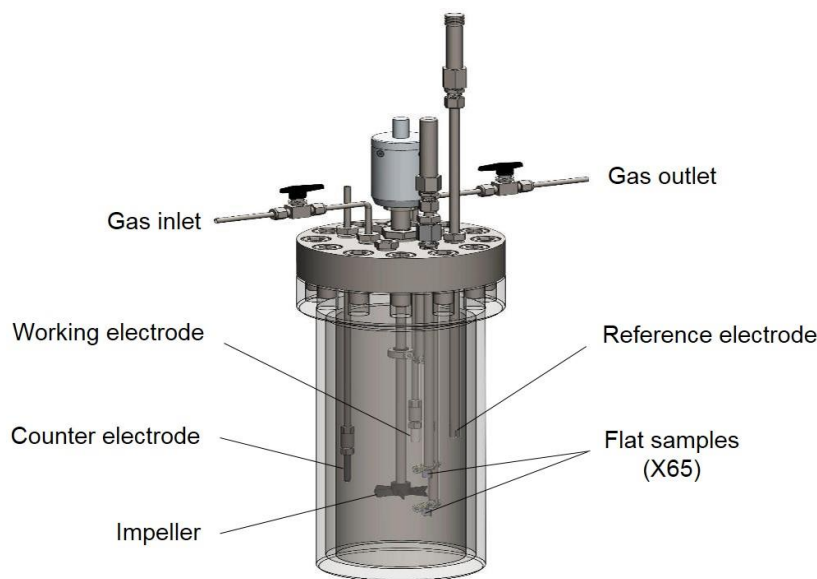


Figure 1 Experimental autoclave set up.

Table 1 Chemical composition of API 5L X65 carbon steel (wt%).

Cr	Mo	S	V	Si	C	P	Ni	Mn	Fe
0.14	0.16	0.009	0.047	0.26	0.13	0.009	0.36	1.16	Balance

The testing parameters and experimental design are shown in Figure 2. The experimental condition was 120°C, 55 bar CO₂ and/or 0.1 bar H₂S, with an initial pH of 5.0 calculated according to an in-house water chemistry model.³⁰ Five separate experiments were conducted. First, experiments with 55 bar CO₂ only and 0.1 bar H₂S only were carried out. Then, a CO₂ and H₂S gas mixture was tested for 4 days at the CO₂/H₂S ratio of 550. Finally, H₂S was added to CO₂ environment after 4 days of exposure and tested for another 4 days, and *vice versa*, to investigate the environment change between sweet and sour conditions on the corrosion behavior of mild steel.

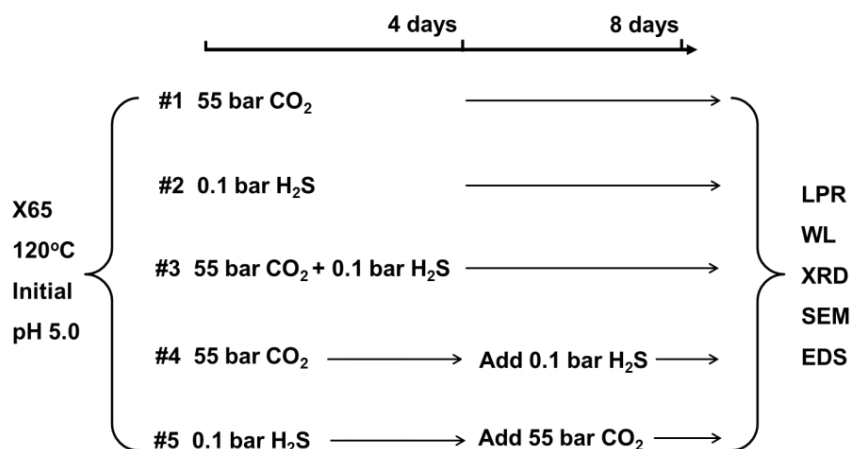


Figure 2 Experimental design.

EXPERIMENTAL RESULTS

Corrosion rates

The LPR corrosion rates of carbon steel in 55 bar pCO₂ and/or 0.1 bar pH₂S environments at 120°C are shown in Figure 3. All the initial corrosion rates were around 10 mm/yr. Then, the corrosion rates quickly decreased down to a stable value in the first day. However, the steady-state corrosion rates varied in different environments. The CO₂-only environment has the lowest stable corrosion rate at approximately 0.15 mm/yr, while the highest stable corrosion rates, about 2 mm/yr, appeared in the H₂S-only environment. In CO₂/H₂S mixture environment, the stable corrosion rate was in between, around 0.7 mm/yr, which is closer to that observed for the CO₂-only environment. When introducing 0.1 bar pH₂S into 55 bar pCO₂ environment, the corrosion rate immediately increased to 0.7 mm/yr, then also quickly decreased back to almost the same value as the one before adding H₂S. Similar behavior was observed when adding CO₂ into an H₂S-only environment.

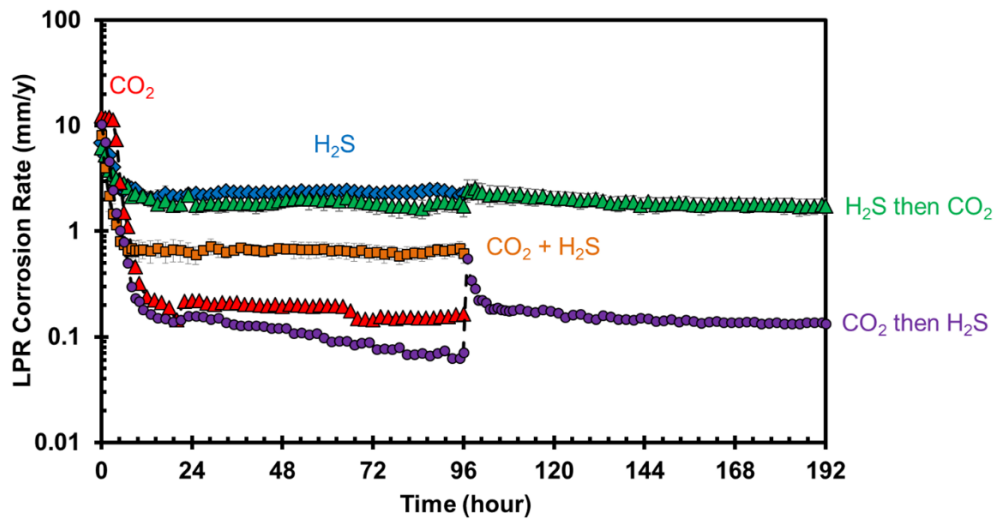


Figure 3 LPR corrosion rate of carbon steel in 55 bar CO₂ and/or 0.1 bar H₂S environments, 120°C, initial pH 5.0, 4 (or 4+4 for H₂S/CO₂ transition experiments) days, $B=23$ mV/decade.

The averaged LPR corrosion rate was compared with WL corrosion rate, as shown in Figure 4. A good agreement can be observed in all the environments by using a B value of 23 mV/decade.

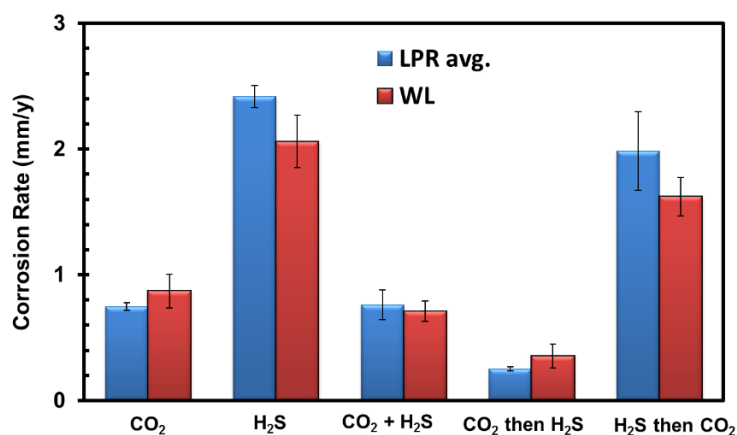


Figure 4 Comparison between average LPR corrosion rate WL corrosion rate, 120°C, 55 bar CO₂ and/or 0.1 bar H₂S, initial pH 5.0, 4 (or 4+4 for H₂S/CO₂ transition experiments) days, $B=23$ mV/decade.

Corrosion products

The corrosion morphologies and cross-sections of steel specimens were examined by XRD and SEM/EDS, as shown in Figure 5 to Figure 11. Pure FeCO₃ formed in the CO₂-only environment. Large bulk FeCO₃ crystals can be observed on the surface. The layer thickness was about 12 μm (Figure 7). In the H₂S-only environment, XRD and SEM show hexagonal pyrrhotite crystals with different sizes covering the steel surface. The cross-section shows there was also an inner Fe₃O₄ layer (~ 25 μm) formed, which was not detected by XRD due to the limited depth of X-ray penetration. The formation of the thermodynamically less stable Fe₃O₄ at high temperature in H₂S environment has been confirmed in various studies.^{16, 30, 31}

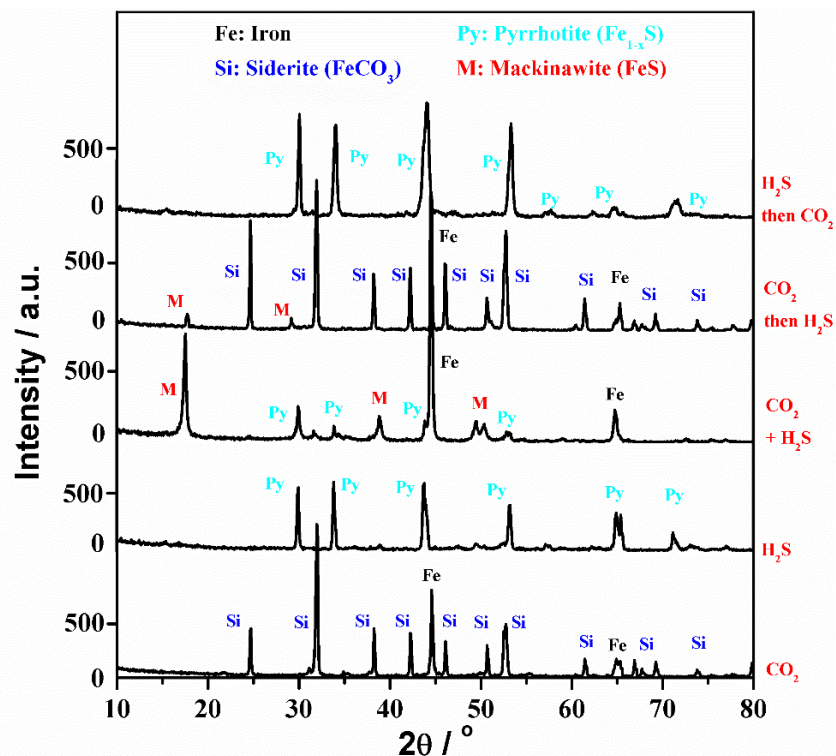


Figure 5 XRD patterns of corrosion products on the steel surface in different environments, 120°C, 55 bar CO₂ and/or 0.1 bar H₂S, initial pH 5.0, 4 (or 4+4 for H₂S/CO₂ transition experiments) days.

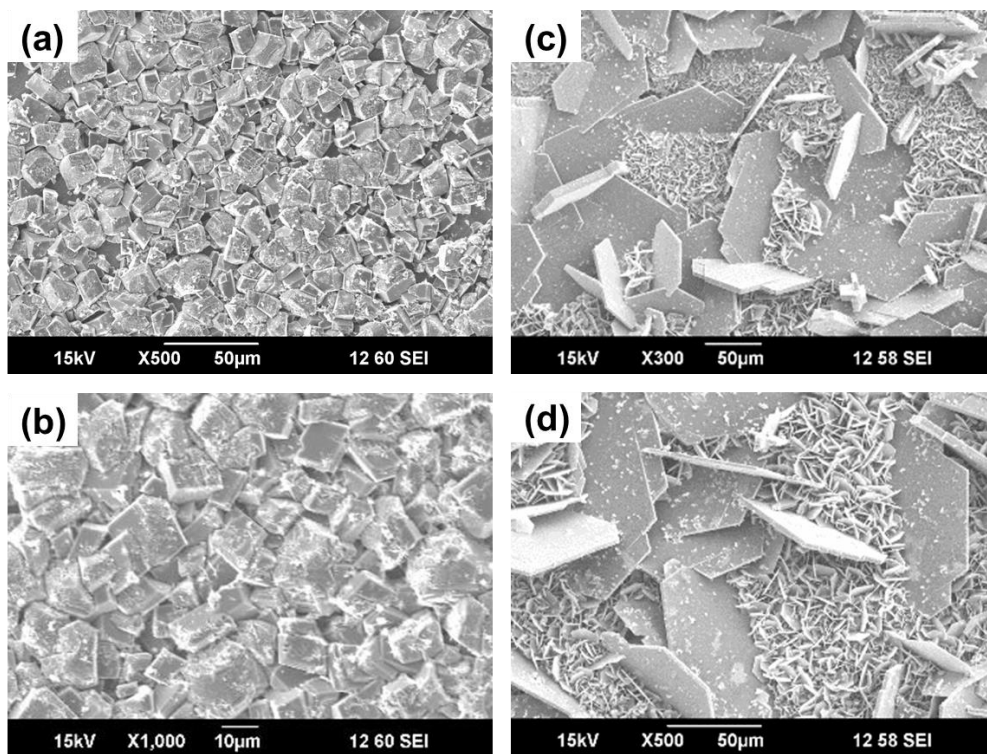


Figure 6 SEM morphologies (a) and (b) 55 bar CO₂, (c) and (d) 0.1 bar H₂S, 120°C, initial pH 5.0, 4 days.

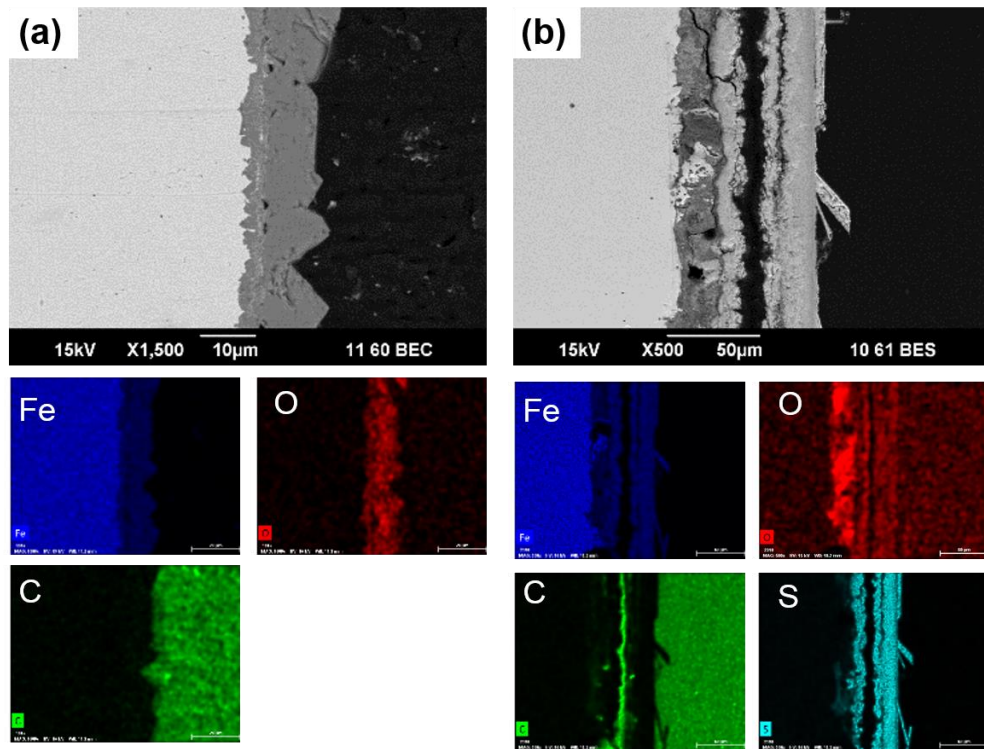


Figure 7 Cross-sections and EDS mapping results (a) 55 bar CO₂, (b) 0.1 bar H₂S, 120°C, initial pH 5.0, 4 days.

In a CO₂ and H₂S mixture environment under the pCO₂/pH₂S ratio of 550, only iron sulfide was observed. The major iron sulfide phase was pyrrhotite with small amount of mackinawite. The pyrrhotite crystals were much smaller and not as dense as observed in the H₂S-only environment. The layer thickness also decreased from tens of microns to less than 5 μm. There was also a thin inner layer (< 0.5 μm) containing oxygen. However, it is not clear if this layer next to the surface is Fe₃O₄ or FeCO₃. In either case, it seems that the high pressure CO₂ (55 bar) could retard Fe₃O₄ formation compared with the H₂S-only experiment. An additional experiment at lower pCO₂=10 bar was performed to confirm this phenomenon, as shown in Figure 8 and Figure 9. Clearly, it can be seen that a thin Fe₃O₄ appeared as the inner layer at a lower pCO₂. The thickness was around 8 μm, which is still below the one formed in H₂S only environment (~ 25 μm). Additionally, the pyrrhotite crystal size and total layer thickness also increased compared with that in 55 bar CO₂ environment.

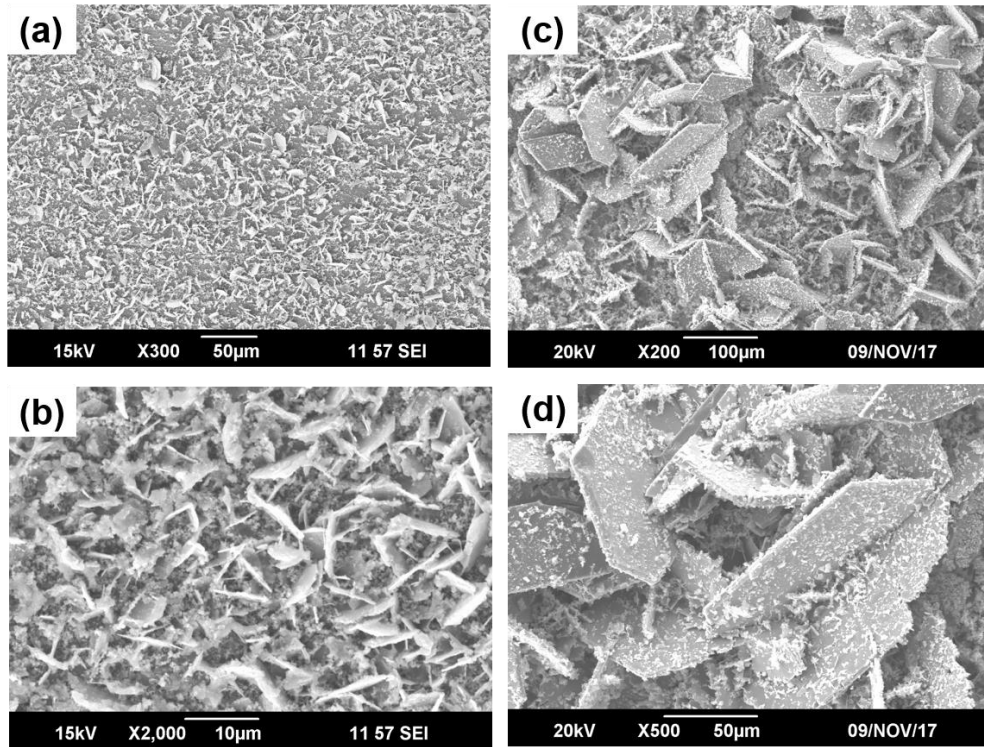


Figure 8 SEM morphologies (a) and (b) 55 bar CO₂ and 0.1 bar H₂S, (c) and (d) 10 bar CO₂ and 0.1 bar H₂S, 120°C, initial pH 5.0, 4 days.

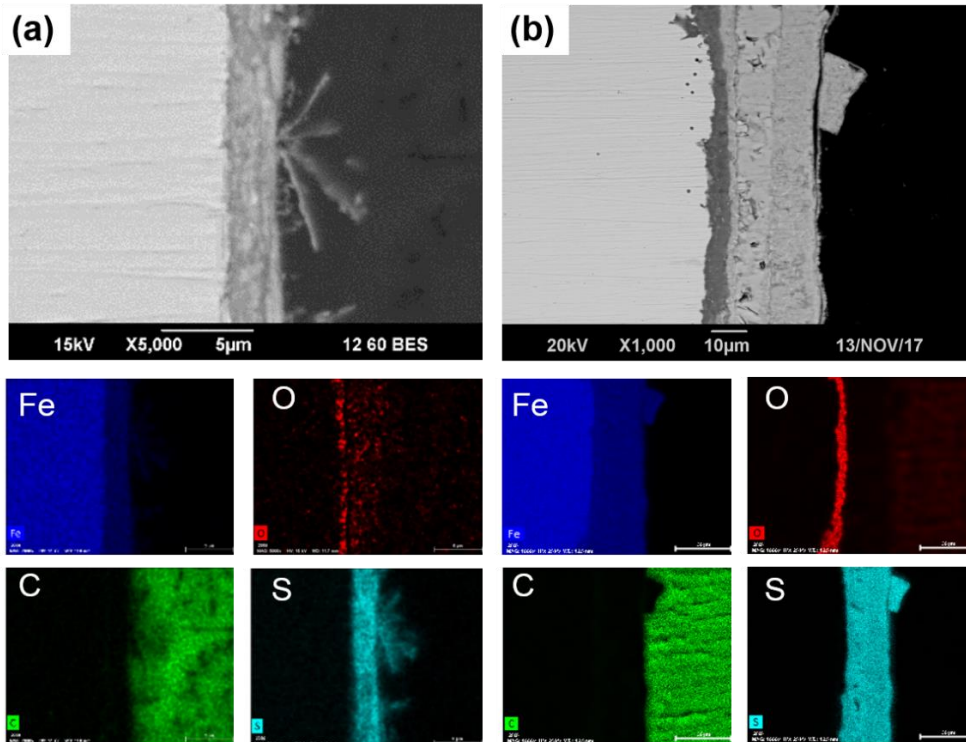


Figure 9 Cross-sections and EDS mapping results (a) 55 bar CO₂ and 0.1 bar H₂S, (b) 10 bar CO₂ and 0.1 bar H₂S, 120°C, initial pH 5.0, 4 days.

In the next experiment, the specimens were tested in 55 bar CO₂-only environment for 4 days; then, 0.1 bar pH₂S was introduced. After days of exposure, some mackinawite could be detected in the XRD pattern, while the major phase was still FeCO₃. It can be seen from Figure 10 that mackinawite precipitated as a thin layer on the void sites within the FeCO₃ layer. EDS mapping results in Figure 11 also confirmed this was a thin sulfide layer formation. In contrast, after adding 55 bar pCO₂ into 0.1 bar pH₂S environment, no obvious change in corrosion product can be observed compared with that in H₂S-only environment. The corrosion products still were constituted of an inner Fe₃O₄ layer and an outer pyrrhotite layer. The only difference between images in Figure 10 and Figure 8 was that most pyrrhotite was observed as larger, bulkier crystals as compared to thin, flaky crystals. This could be due to the increase of exposure time (8 days vs. 4 days).

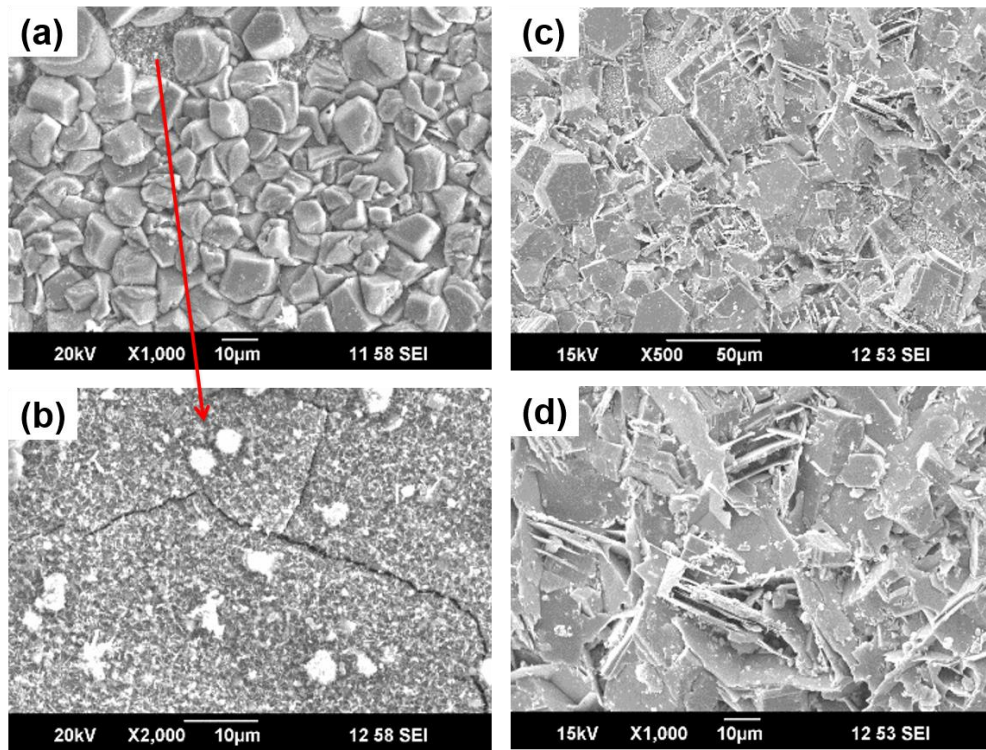


Figure 10 SEM morphologies (a) and (b) 55 bar CO₂ then adding 0.1 bar H₂S, (c) and (d) 0.1 bar H₂S then adding 55 bar CO₂, 120°C, initial pH 5.0, 4 + 4 days.

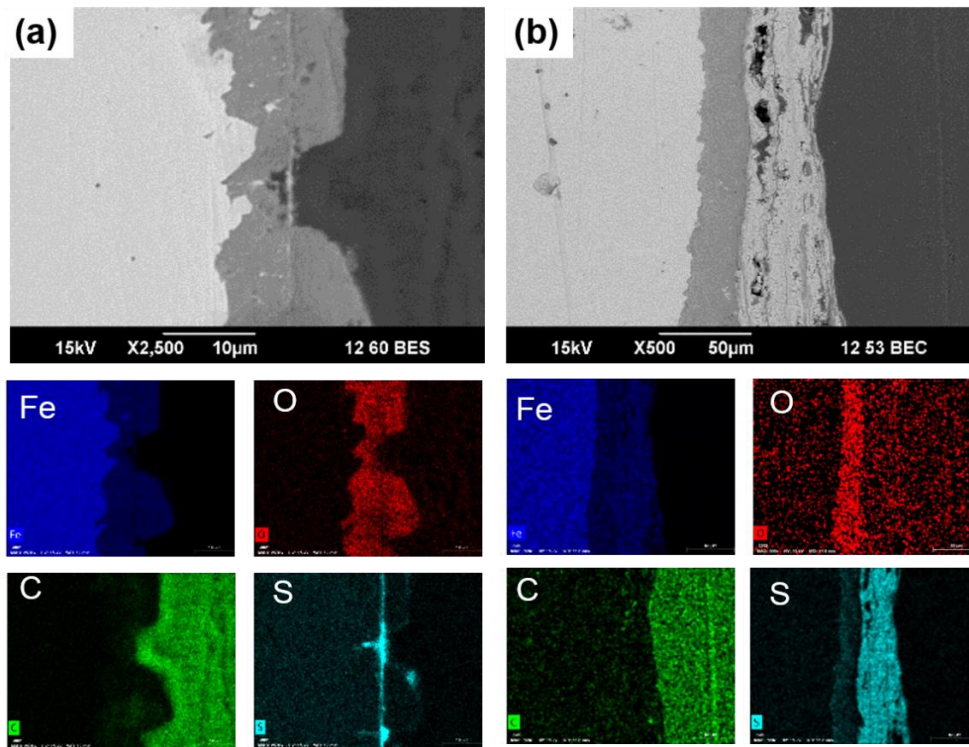


Figure 11 Cross-sections and EDS mapping results (a) 55 bar CO₂ then adding 0.1 bar H₂S, (b) 0.1 bar H₂S then adding 55 bar CO₂, 120°C, initial pH 5.0, 4+4 days.

Surface profilometry

The surface profilometry of the steel was examined after removing the corrosion products. The typical images are shown in Figure 12. No obvious localized corrosion was observed for this series of experiments (Figure 2). Therefore, all were considered as uniform corrosion in the tested CO₂ and/or H₂S environments, which is in good agreement with the previous study.³⁰

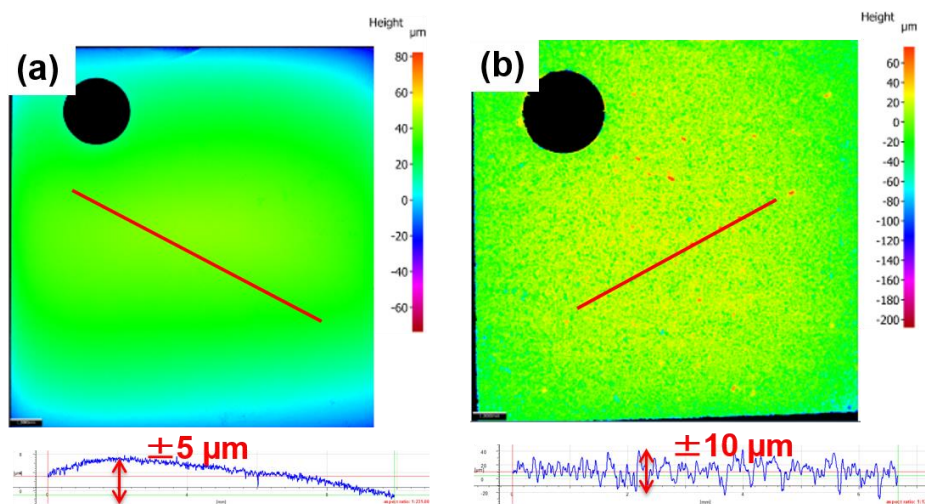


Figure 12 Surface profilometry after removing corrosion products (a) 55 bar CO₂ then adding 0.1 bar H₂S, (b) 0.1 bar H₂S then adding 55 bar CO₂, 120°C, initial pH 5.0, 4 + 4 days.

DISCUSSION

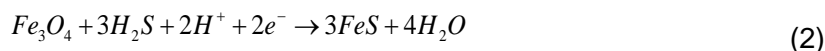
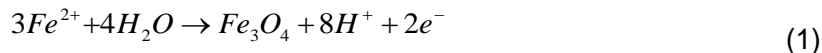
CO₂/H₂S ratio

According to Figure 5, Figure 8, Figure 9, iron sulfide mainly formed in the CO₂ and H₂S mixture environment with partial pressures under the pCO₂/pH₂S ratio of 550 at 120°C. The corrosion product was still dominated by H₂S. Obviously, the 500 ratio as a transition point between CO₂ and H₂S corrosion is not valid at this high temperature. However, it does not mean only H₂S corrosion mitigation must be taken without the consideration of CO₂. The corrosion rate also should be considered, as shown in Figure 3. Yet, the corrosion rate in the mixed CO₂ and H₂S environment was much closer to that in a CO₂-only environment (Figure 3), which could suggest that the corrosion rate was controlled by CO₂ even though no FeCO₃ corrosion product was detected. Anyhow, the use of the 500 pCO₂/pH₂S ratio for making important decisions should be applied with strong caution in the oil and gas industry and further investigation under different conditions is required.

Role of the Fe₃O₄ layer

In most cases, the corrosion rate could be closely related to the corrosion product layer formation. Comparing H₂S-only and CO₂/H₂S mixture (10 bar and 55 bar pCO₂) experiments, the thickness of the inner Fe₃O₄ layer decreased from 25 μm to essentially zero. It can be concluded that high pressure CO₂ can retard Fe₃O₄ formation at high temperature in H₂S environment. Meanwhile, the corrosion rate followed a similar decreasing trend, from 2 mm/yr to 0.7 mm/yr (Figure 3). It seems that Fe₃O₄ layer was not protective in the H₂S-only environment. However, without H₂S, Fe₃O₄ was shown to be very protective layer³¹ at high temperature, with a stable corrosion rate below 0.4 mm/yr.

Therefore, the high corrosion rate must also be related to the presence of the iron sulfide layer. Since Fe₃O₄ is thermodynamically less stable than iron sulfide, it has been demonstrated that Fe₃O₄ continuously forms at the steel/Fe₃O₄ interface, and converts to iron sulfide at the Fe₃O₄/FeS interface via Reaction (1) and (2).³¹



Effect of environment change

When H₂S was injected into CO₂ environment, the LPR corrosion rate increased from 0.15 mm/yr to 0.7 mm/yr. The rise was also observed when CO₂ was injected to an H₂S-only environment (Figure 3). This could be attributed to the pH decreasing with acid gas injection. The corrosion rate is hypothesized to quickly decrease back to the previous level due to the presence of already formed FeCO₃ or Fe₃O₄/FeS layer. Therefore, the environmental change had almost no effect on the steady corrosion rate once the original corrosion product has formed. After another 4 days, iron sulfide (mackinawite) precipitated when H₂S was added to the CO₂ environment while no FeCO₃ precipitation was observed when CO₂ was added to the H₂S environment, as iron sulfide is more kinetically and thermodynamically favored than FeCO₃ under the testing conditions.^{32,33} However, longer term experiments are necessary to determine whether the FeCO₃ layer will convert to FeS and consequently affect the general and localized corrosion rates.

CONCLUSIONS

The corrosion behavior of mild steel in 55 bar pCO₂ and/or 0.1 bar pH₂S environment at high temperature was studied for the first time. The main conclusions can be drawn as follows:

- The CO₂/H₂S ratio of 500 as the transition point between CO₂ and H₂S corrosion is not valid at high temperature. The corrosion products were still dominated by H₂S under the CO₂/H₂S ratio of 550. Industrial application of this ratio needs more investigation.
- High pressure CO₂ can retard Fe₃O₄ formation in H₂S environment. The high corrosion rate in an H₂S-only environment could be related to the continuous Fe₃O₄ formation and conversion to FeS.
- No obvious change in steady state corrosion rate was observed when the environment was switched from sweet (CO₂) to sour (H₂S) and *vice versa* in short term experiments.

ACKNOWLEDGEMENTS

The author also would like to thank the following companies for their financial support: Anadarko, Baker Hughes, BP, Chevron, CNOOC, ConocoPhillips, DNV GL, ExxonMobil, M-I SWACO (Schlumberger), Multi-Chem (Halliburton), Occidental Oil Company, PTT, Saudi Aramco, SINOPEC (China Petroleum), and TOTAL.

REFERENCES

1. C.A. Palacios, J.R. Shadley, "Characteristics of Corrosion Scales on Steels in a CO₂-Saturated NaCl Brine," *Corrosion* 47, 2(1991): p. 122-127.
2. Y. Choi, S. Netic, S. Ling, "Effect of H₂S on the CO₂ corrosion of carbon steel in acidic solutions," *Electrochimica Acta* 56, 4(2011): p. 1752-1760.
3. N. Zhang, D. Zeng, G. Xiao, J. Shang, Y. Liu, D. Long, Q. He, A. Singh, "Effect of Cl- Accumulation on Corrosion Behavior of Steels in H₂S/CO₂ Methyl-diethanolamine (MDEA) Gas Sweetening Aqueous Solution," *Journal of Natural Gas Science and Engineering* 30, (2016): p. 444-454.
4. G. DeBruijn, "High-pressure, High-temperature Technologies," *Oilfield Review*, (2008): p. 46-60.
5. S. Gao, C. Dong, A. Fu, K. Xiao, X. Li, "Corrosion Behavior of the Expandable Tubular in Formation Water," *International Journal of Minerals, Metallurgy, and Materials* 22, 2(2015): p. 149-156.
6. S. Huizinga, "Technical Note: A Review of Assessment of H₂S Environmental Severity in Field and Lab—Why Use Fugacity?" *Corrosion* 73, 4(2017): p. 417-425
7. S. Netic, J. Postlethwaite, S. Olsen, "An Electrochemical Model for Prediction of Corrosion of Mild Steel in Aqueous Carbon Dioxide Solutions," *Corrosion* 52, 4(1996): p. 280-294.
8. A. Kahyarian, M. Singer, S. Netic, "Modeling of Uniform CO₂ Corrosion of Mild Steel in Gas Transportation Systems: A Review," *Journal of Natural Gas Science and Engineering* 29, (2016): p. 530-549.
9. J. Ning, Y. Zheng, B. Brown, D. Young, S. Netic, "A Thermodynamic Model for the Prediction of Mild Steel Corrosion Products in an Aqueous Hydrogen Sulfide Environment," *Corrosion* 71, 8(2015): p. 945-960.
10. Y. Zheng, J. Ning, B. Brown, S. Netic, "Advancement in Predictive Modeling of Mild Steel Corrosion in CO₂-and H₂S-Containing Environments," *Corrosion* 72, 5(2016):p. 679-691.
11. A.K. Dunlop, H.L. Hassell, P.R. Rhodes, "Fundamental Considerations in Sweet Well Corrosion," CORROSION/1983, paper no. 46 (Anaheim, CA: NACE, 1983).
12. R. Nyborg, "Guidelines for prediction of CO₂ corrosion in oil and gas production systems," IFE/KR/E-2009/003.
13. "Wet Gas Internal Corrosion Direct Assessment Methodology for Pipelines," NACE TG 305, 2010.
14. S.N. Smith, "The Carbon Dioxide/Hydrogen Sulfide Ratio—Use and Relevance," *Materials Performance* 54, 5(2015): p. 2-5.
15. T. Tanupabrungsun, B. Brown, S. Netic, "Effect of pH on CO₂ Corrosion of Mild Steel at Elevated Temperatures," CORROSION/2013, paper no. 2348 (Orlando, FL: NACE, 2013).

16. S. Gao, P. Jin, B. Brown, D. Young, S. Nescic, M. Singer, "Effect of High Temperature on the Aqueous H₂S Corrosion of Mild Steel," *Corrosion* 73, 10(2017): p. 1188-1191.
17. S. Gao, B. Brown, D. Young, M. Singer, "Formation of iron oxide and iron sulfide at high temperature and their effects on corrosion," *Corrosion Science* 135, (2018): p. 167-176.
18. S. Gao, B. Brown, D. Young, S. Nescic, M. Singer, "A Modified Thermodynamic Model for the Prediction of Mild Steel Corrosion Product Formation at High Temperature in an Aqueous H₂S Environment," CORROSION/2019, paper no. 12869 (Nashville TN: NACE, 2019).
19. B. Mishra, S. Al-Hassan, D.L. Olson, M.M. Salama, "Development of a Predictive Model for Activation-Controlled Corrosion of Steel in Solutions Containing Carbon Dioxide," *Corrosion* 53, 11(1997): p. 852-859.
20. Z. Yin, Y. Feng, W. Zhao, Z. Bai, G. Lin, "Effect of Temperature on CO₂ Corrosion of Carbon Steel," *Surface and Interface Analysis* 41, 6(2009): p. 517-523.
21. J. Kvarekval, A. Dugstad, I.H. Omar, Y. Gunaltun, "H₂S Corrosion of Carbon Steel under Simulated Kashagan Field Conditions," CORROSION/2005, paper no. 05300 (Houston, TX: NACE, 2005).
22. Y. Qi, H. Luo, S. Zheng, C. Chen, Z. Lv, M. Xiong, "Effect of Temperature on the Corrosion Behavior of Carbon Steel in Hydrogen Sulphide Environments," *International Journal of Electrochemical Science* 9, (2014): p. 2101-2112.
23. G. Zhao, X. Lu, J. Xiang, Y. Han, "Formation Characteristic of CO₂ Corrosion Product Layer of P110 Steel Investigated by SEM and Electrochemical Techniques," *Journal of Iron and Steel Research International* 16, 4(2009): p. 89-94.
24. J. Kvarekval, R. Nyborg, H. Choi, "Formation of Multilayer Iron Sulfide Films During High Temperature CO₂/H₂S Corrosion of Carbon Steel," CORROSION/2003, paper no. 03339 (San Diego, CA: NACE, 2003).
25. R. Elgaddafi, R. Ahmed, S. Shah, "Modeling and Experimental Studies on CO₂-H₂S Corrosion of API Carbon Steels under High-pressure," *Journal of Petroleum Science and Engineering* 156, (2017): p. 682-696.
26. Z. Liu, X. Gao, L. Du, J. Li, P. Li, X. Bai, R. D. K. Misra, "Corrosion Behavior of Low-Alloy Pipeline Steel Exposed to H₂S/CO₂-Saturated Saline Solution," *Journal of Materials Engineering and Performance* 26, (2017): p. 1010-1017.
27. Y. Liu, Z. Zhang, N. Bhandari, F. Yan, F. Zhang, G. Ruan, Z. Dai, H.A. Alsaiani, A.Y. Lu, G. Deng, A.T. Kan, M. B. Tomson, "Iron Sulfide Precipitation and Deposition under Different Impact Factors," 2017 SPE International Conference on Oilfield Chemistry, SPE-184546-MS (Montgomery, TX: SPE, 2017).
28. Y. Xiong, D. Fischer, F. Cao, J. Pacheco, "Impact of Pre-Corrosion on Corrosion Inhibitor Performance: Can We Protect Aged Pipelines," CORROSION/2017, paper No. 8919 (New Orleans, LA: NACE, 2017).
29. Y. R. Thodla, F. Gui, K. Evans, C. Joia, I.P. Baptista, "Corrosion Fatigue Performance of Super 13 CR, Duplex 2205 and 2507 for Riser Applications," CORROSION/2010, paper No. 312 (Houston, TX: NACE, 2010).
30. S. Gao, P. Jin, B. Brown, D. Young, S. Nescic, M. Singer, "Corrosion Behavior of Mild Steel in Sour Environments at Elevated Temperatures," *Corrosion* 73, (2017): p. 915-926.
31. S. Gao, B. Brown, D. Young, S. Nescic, M. Singer, "Formation Mechanisms of Iron Oxide and Iron Sulfide at High Temperature in Aqueous H₂S Corrosion Environment," *Journal of The Electrochemical Society* 165, 3(2018): p. C171-C179.
32. T. Tanupabrungsun, D. Young, B. Brown, S. Nescic, "Construction and Verification of Pourbaix Diagrams for CO₂ Corrosion of Mild Steel Valid up to 250°C," CORROSION/2012, paper no. 0001418 (Salt Lake City, UT: NACE, 2012).
33. J. Ning, Y. Zheng, B. Brown, D. Young, S. Nescic, "Construction and Verification of Pourbaix Diagrams for Hydrogen Sulfide Corrosion of Mild Steel," CORROSION/2015, paper no. 5507 (Dallas, TX: NACE, 2015).